

THE THEORETICAL ASTROPHYSICAL OBSERVATORY[†]: CLOUD-BASED MOCK GALAXY CATALOGUES

MAKSYM BERNYK¹, DARREN J. CROTON¹, CHIARA TONINI^{2,1}, LUKE HODKINSON¹, AMR H. HASSAN¹, THIBAUT GAREL^{3,1},
ALAN R. DUFFY¹, SIMON J. MUTCH^{2,1}, GREGORY B. POOLE^{2,1}, SARAH HEGARTY¹

¹Centre for Astrophysics & Supercomputing, Swinburne University of Technology, PO Box 218, Hawthorn, Victoria, 3122, Australia

²School of Physics, University of Melbourne, Parkville, Victoria 3010, Australia and

³Centre de Recherche Astrophysique de Lyon, Université de Lyon, Université Lyon 1, CNRS, Observatoire de Lyon, 9 avenue Charles André, 69561 Saint-Genis Laval Cedex, France

Draft version January 25, 2016

ABSTRACT

We introduce the Theoretical Astrophysical Observatory (TAO), an online virtual laboratory that houses mock observations of galaxy survey data. Such mocks have become an integral part of the modern analysis pipeline. However, building them requires an expert knowledge of galaxy modelling and simulation techniques, significant investment in software development, and access to high performance computing. These requirements make it difficult for a small research team or individual to quickly build a mock catalogue suited to their needs. To address this TAO offers access to multiple cosmological simulations and semi-analytic galaxy formation models from an intuitive and clean web interface. Results can be funnelled through science modules and sent to a dedicated supercomputer for further processing and manipulation. These modules include the ability to (1) construct custom observer light-cones from the simulation data cubes; (2) generate the stellar emission from star formation histories, apply dust extinction, and compute absolute and/or apparent magnitudes; and (3) produce mock images of the sky. All of TAO's features can be accessed without any programming requirements. The modular nature of TAO opens it up for further expansion in the future.

Subject headings: galaxy formation, mock catalogue, light cone, online tools, cloud computing

1. INTRODUCTION

Astronomy has entered an era of survey science, thanks almost solely to instruments and telescopes that can sample unprecedented volumes of the cosmos with unparalleled sensitivity out to great distances. Riding this wave, the field of galaxy formation and evolution has grown to become one of the most active research areas in astrophysics. Progress feeds off progress, where increasingly detailed observations of galaxies are used to build new theories, that in turn lead to predictions, which can direct and be tested against new observations. As the instruments have increased in sophistication, so have the amount of data they collect. Similarly, simulations of galaxies and the Universe have grown to keep pace.

It is thus not surprising that data access has become a signature of this new era. Internet and cloud technologies allow scientists to store and retrieve large scientific datasets remotely. This is sometimes necessary since data volume and complexity often require resources beyond what is locally available. But even when not necessary it is frequently desired, as relocating storage and processing off-site reduces overheads, simplifies data management, and facilitates data sharing.

Two notable examples are the Sloan Digital Sky Survey (SDSS, Abazajian et al. 2003) “SkyServer”, which hosts imaging, spectra, spectroscopic and photometric data; and the German Astrophysical Virtual Observatory (GAVO, Lemson & Virgo Consortium 2006), which houses the Millennium Simulation theoretical data products. Both on-line repositories are accessible by means of the Structured Query Language (SQL), and due to their accessibility, both have vastly increased the scien-

tific value of the data they hold through data re-use. There are many ways this benefit can be measured, arguably the most important being an increased number of scientific publications. Such publications come predominantly from researchers who had nothing to do with the original data production.

In large part due to this ease of access, the division between observer and theorist has faded somewhat. Observers now routinely use cutting edge theoretical models in their analysis, and theorists compare model predictions against observational data. This has all meant that the modern astronomer now routinely works across many traditional boundaries, often combining multiple disparate data products to undertake their science.

The focus of the present work is on access to theoretical survey data, such as cosmological-scale dark matter simulations and galaxy formation models. Many groups around the world are currently producing state-of-the-art theory products whose value to the community is immense. However access from outside the group is often prohibitive, even when the authors are happy for others to use their work. Furthermore, comparing different simulations and models on an equal footing can be extremely problematic due to data size and transport barriers, data format differences, and complexity. This makes understanding how to correctly use the data challenging for the non-expert.

Access is but one part of the puzzle however. To be compared fairly to observations, simulations must typically be modified to look more like the data being compared against. This can include: mapping the simulation cube into an observed light-cone where distance also equates to time evolution in the simulation, calculating absolute and apparent magnitudes for model galaxies in

[†] <https://tao.asvo.org.au/>

select filters from their star formation and metallicity histories, and “observing” mock galaxies to generate images similar to that which would be collected by a CCD. All are non-trivial tasks that require great care to implement correctly.

Some effort has already gone in to producing such tools for the community. For example, the Mock Map Facility (MoMAF, Blaizot et al. 2005) allows a user to build mock galaxy catalogues using the GALICS semi-analytic model (Blaizot et al. 2004). In a similar fashion, the Millennium Run Observatory (Overzier et al. 2013) provides a powerful set of tools to access and visualise mock catalogues based on the Millennium Run suite of dark matter simulations (Springel 2005).

In this paper we present a new online tool – the Theoretical Astrophysical Observatory (TAO) – that aims to further address the problem of community data access and, more specifically, simplifies the process of building mock galaxy catalogues to more individualised specifications. This paper is structured as follows: An introduction to TAO is presented in Section 2. In the subsequent sections we then describe the first four TAO science modules: the basic galaxy and simulation selection tools (Section 3), the light-cone module (Section 4), the spectral energy distribution (SED) module (Section 5), and the mock image generation module (Section 6). We then explore usage cases in Section 7 that demonstrate the utility and functionality of TAO. Section 8 concludes with a summary.

For all results presented the cosmology of the simulation from which the result was drawn is assumed unless otherwise indicated, and we refer the reader to the associated reference for further details.

2. THE THEORETICAL ASTROPHYSICAL OBSERVATORY - AN OVERVIEW

The Theoretical Astrophysical Observatory (TAO) provides web access to cloud-based¹ mock extragalactic survey data, generated using sophisticated semi-analytic galaxy formation models that are coupled to large N-body cosmological simulations. TAO is designed to be flexible, so that different simulations and models can be stored and accessed from a single location with a consistent data format. The interface for TAO is clean and built with simplicity in mind. All of TAO’s features require no programming knowledge to use, maximising accessibility to astronomers, be they observers or theorists.

A major feature of TAO is its ability to post-process the hosted data for different scientific applications. This is achieved through a number of science modules that can be chained in user-specified configurations, depending on the desired requirements of the astronomer and the module functionality. In addition, this modular design makes TAO readily expandable with new functionality in the future.

- *Simulation data module.* This core module provides direct access to the original simulation and semi-analytic galaxy formation model data stored in the TAO SQL database. The user can specify

the desired galaxy and dark matter halo properties to be retrieved at an epoch of interest from the simulation box (see Section 3).

- *Light-cone module.* This module remaps the spatial and temporal distribution of galaxies in the original simulation box on to that of the observer light-cone. The parameters of the cone are user configurable (see Section 4).
- *Spectral energy distribution module (SED).* This module retrieves the star formation and metallicity histories for each galaxy (either in the box or cone) from the TAO database and applies a user-selected stellar population synthesis model and dust model to produce individual galaxy spectra. These spectra are convolved with a set of filters to compute both apparent and absolute magnitudes (see Section 5).
- *Image module.* This module takes the output of both the light-cone and SED modules to construct user defined mock images. Images can be customised using a range of properties, such as sky area, depth, and observed filter (see Section 6).

In Figure 1 we show a broad overview of the TAO infrastructure. At the top level we define the connection between the account based user interface and user database. In the middle level the various science modules are shown, as introduced above and which will be described in more detail in the subsequent sections. Both public and private data storage, containing the dark matter simulations, galaxy data, photometry etc., are shown in the lower level. On the back-end TAO is supported by a scalable database cluster hosted on the gSTAR supercomputer² at the Swinburne University of Technology. Each component of TAO affects the user experience and workflow, speed of mock data generation and retrieval, and the quality and utility of the final mock catalogue.

Users interact with TAO through a simple web form, where they can select a dark matter simulation, galaxy formation model, a box or cone geometry, and the associated parameters which define each. The desired galaxy and simulation properties to be included in the mock, including both absolute and apparent magnitudes in various filters, are all specified by the user. These selections are then passed to the back-end science modules via an XML parameter file, which can also be retrieved from the web interface for reference or later resubmission. Any required computations, e.g. to build a light-cone or set of SEDs, are then triggered on the gSTAR supercomputer for processing. The user is notified via email when their mock catalogue is completed, which may take from minutes to many hours depending on the size of the task. TAO offers a choice of output formats, including CSV, HDF5 and FITS. The final mock catalogue can then be downloaded directly from the TAO website “History” tab to the user’s local machine. More advanced SQL/ADQL querying of the data is accessible through a VO Table Access Protocol (TAP) client, such as TOPCat.

In Figure 2 we show the TAO web interface, highlighting its minimalist yet functional design. The user interface design objective is to provide a simple portal that

¹ In this paper we define the “cloud” as Infrastructure as a Service (IaaS), which includes data storage and access, software infrastructure, and the use of supercomputer facilities.

² <http://www.astronomy.swin.edu.au/supercomputing/>

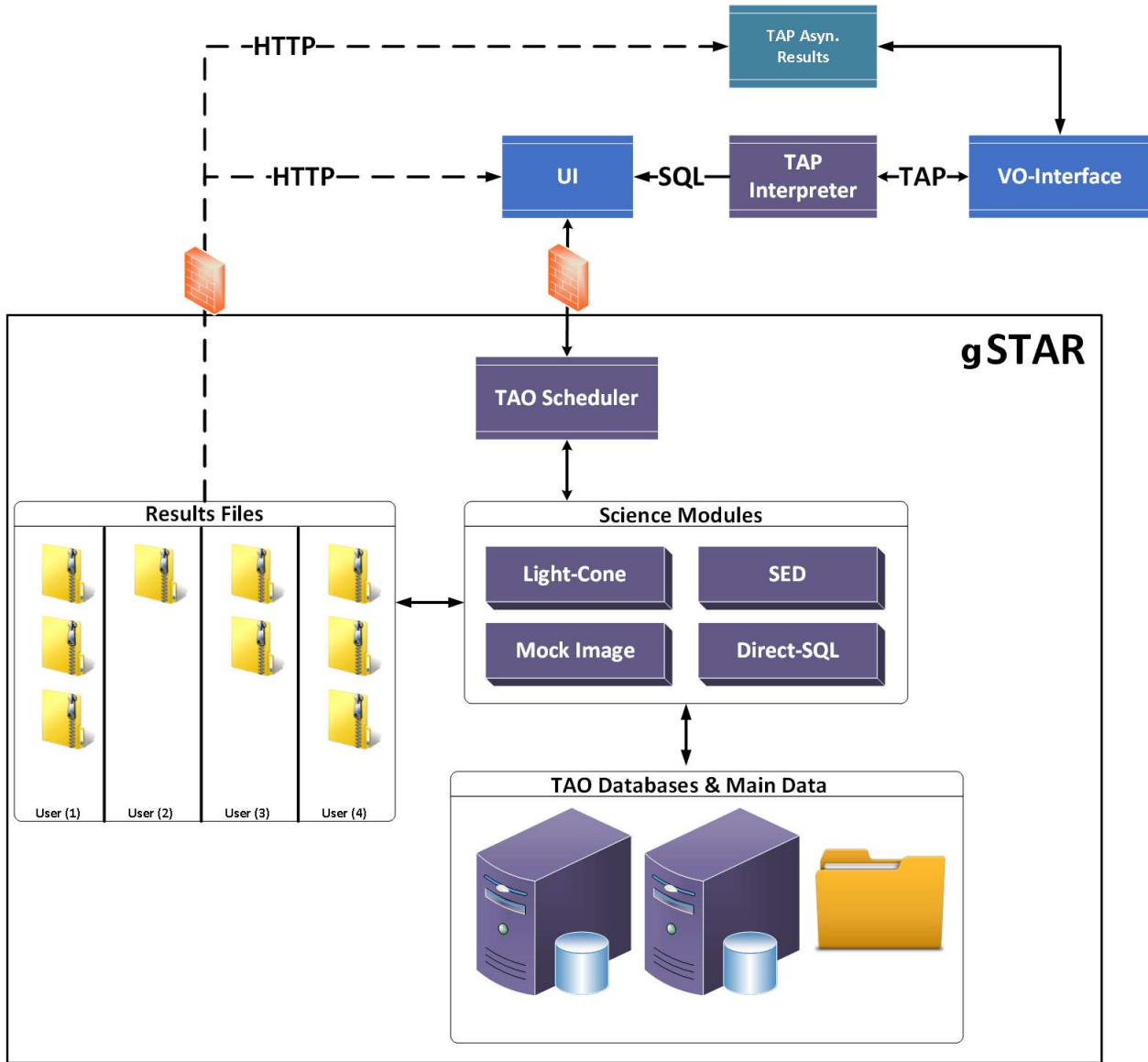


FIG. 1.— A TAO architecture diagram. The main TAO database, science modules, and results storage space are located on the gSTAR supercomputer at Swinburne University. The user interface and Table Access Protocol (TAP) server are hosted on a separate web server and accept job requests. Jobs are queued on the supercomputer via the jobs scheduler. Upon the job completion results are available for download over the internet.

makes using the science modules easy and intuitive. In the spirit of reaching as many astronomers as possible, no programming knowledge (SQL or other) is required to use any part of TAO, keeping the barrier for access low.

TAO is part of the larger All-Sky Virtual Observatory (ASVO) project³, whose goal is to federate astronomy data and serve this to the wider community via the cloud. The ASVO constitutes a major infrastructure investment that links observational data with theoretical capabilities. It establishes a platform from which astronomers can optimally access and exploit the exponential growth in astronomical data volume in the coming decade. As a first release, the ASVO will include cloud access to the SkyMapper data archives (Keller et al. 2007), in addi-

tion to the simulated data provided through TAO. Ultimately it is expected that the ASVO will incorporate data at multiple wavelengths, including radio observations from the upcoming Australian Square Kilometre Array Pathfinder (ASKAP) telescope (Johnston et al. 2008).

3. THE GALAXY AND SIMULATION MODULE

Simulated galaxy data is the core product of TAO. Hence, it is useful to review the basics of how TAO data is generated and the properties that define it. We do this by considering dark matter simulations and semi-analytic galaxy modelling in turn. More detail on these methods can be found in Baugh (2006); Croton et al. (2006); Benson (2012). We also clarify some of the technical requirements of TAO to hold and use this data. These include the requisite data format and minimum

³ <http://www.asvo.org.au/>

ASVO TAO *(Beta)*
New Catalogue
History
Admin
Documentation
Support

New Catalogue (Required Fields are marked with an asterisk)

Job Type
General Properties
Spectral Energy Distribution
Mock Image
Selection
Output format
Summary and submit

Data Selection

Catalogue geometry *

Dark matter simulation *

Galaxy model *

Right Ascension Opening Angle (degrees) *

Declination Opening Angle (degrees) *

Redshift Min *

Redshift Max *

Estimated job size: 2%

Unique
 Random

Select the number of light-cones: *

maximum is 3

Output properties

Output properties *

Available

- Galaxy Masses**
- Bulge Stellar Mass
- Cold Gas Mass
- Hot Gas Mass
- Ejected Gas Mass
- Intracluster Stars Mass
- Metals Total Stellar Mass
- Metals Bulge Mass
- Metals Cold Gas Mass
- Metals Hot Gas Mass
- Metals Ejected Gas Mass

Selected

- Galaxy Masses**
- Total Stellar Mass
- Black Hole Mass
- Positions & Velocities**
- Right Ascension
- Declination
- Redshift (Cosmological)
- Redshift (Observed)

Selected simulation details

Millennium

Cosmology: WMAP-1
 Cosmological parameters: $\Omega_m = 0.25$,
 $\Omega_\Lambda = 0.75$, $\Omega_b = 0.045$, $\sigma_8 = 0.9$, $h = 0.73$, $n = 1$
 Box size: 500 Mpc/h
 Mass resolution: 8.6×10^8 Msun/h
 Force resolution: 5 kpc/h
 Paper: Springel et al. 2005

Selected galaxy model details

SAGE

Kind: semi-analytic model
 Paper: Croton et al. 2006

Selected output property details

Black Hole Mass (10+10solMass/h)

Supermassive black hole mass

< Previous
Next >

FIG. 2.— The TAO web interface, showing how complex queries can be generated through a simple selection of galaxy and simulation properties, plus additional options to access the various science modules.

galaxy and halo properties required by the core and higher-level science modules. An up-to-date list of the data hosted can be found at the TAO website⁴.

3.1. Dark matter simulations and large-scale structure

An efficient way to simulate the universe inside a supercomputer is to focus on the dominant mass distribution and its evolution. This usually involves running a collisionless N-body simulation in a volume that is large enough to be representative of the Universe as a whole, and provides a significant reduction in computational effort at fixed resolution compared with hydrodynamic galaxy formation simulations. Hydrodynamic effects are complicated and slow to compute numerically relative to the rather simple calculations required in a gravity-only simulation. Hence, gas and galaxies are often added later in post-processing using semi-analytic or other statistical techniques (see below).

As the universe evolves gravity pulls small structures together to assemble larger structures (i.e. hierarchical growth). Within the numerical simulation, such “halos” are typically identified using a Friends-of-Friends (FoF) algorithm (Davis et al. 1985; Springel et al. 2001; More et al. 2011), which detects gravitationally bound systems of particles and determines their properties. Structures within structures (i.e. sub-structures) can be found using a variety of methods (e.g. Springel et al. 2005; Behroozi, Wechsler & Wu 2013). Such sub-structures are typically expected to host the smaller satellite galaxies and are subservient to the larger halo and central galaxy at the halo centre.

This information, calculated across all time-steps in a simulation for a particular object, defines its merger tree. The collection of such trees is then used as input to construct a galaxy formation model. An example halo merger tree from the Millennium Simulation (Springel et al. 2005) is shown in Figure 3. Here, the top panel shows the tree itself for a $1.9 \times 10^{13} M_{\odot}$ halo at $z = 0$ (assuming $h = 0.73$), while the corresponding mass growth history with time is shown in the lower panel.

Simulations are run for different science goals, and each allow the exploration of different physics depending on how they were set-up. TAO provides the user with a choice of dark matter simulations, run with various sizes, mass resolutions and cosmological parameters.

3.2. Modelling the evolution of galaxies

There are a number of ways to model the evolution of a galaxy inside a dark matter halo. For the higher-level science modules, TAO requires the galaxies in its database to have a minimum set of properties. As discussed below in Section 3.3, each galaxy record in the TAO database should contain information about its position, merger history, and star formation history. So, at a minimum, the methodology used to generate the galaxy population must produce this information.

The best suited methodology for this purpose is that of semi-analytics (White & Frenk 1991). Semi-analytic models not only calculate all the required properties for galaxies, but also link their evolution over time using the

halo merger trees to follow the growth histories. Note that any other method that produces the minimum set of properties is also acceptable; we focus on semi-analytics here as it is the most common and nicely illustrates the requirements of the TAO system.

A semi-analytic galaxy model takes as input a dark matter halo merger tree and evolves its baryonic content with time using prescriptions that describe the phenomenology of each key galaxy formation process.

1. As a dark matter halo grows its potential well gets deeper and hence attracts baryons in the form of diffuse gas from the surrounding medium.
2. This gas cools, conserving angular momentum as it falls to the centre of the halo and forms a rotationally supported disk.
3. Within this flattened disk stars begin to form. A galaxy is born.
4. Each episode of star formation results in a distribution of stellar masses sampled from the initial mass function.
5. The most massive stars are short-lived and explode as supernovae, injecting metals and energy back into the interstellar and intergalactic medium.
6. Galaxies merge as hierarchical growth proceeds, resulting in morphological evolution and the birth of super-massive black holes.
7. Supernova and super-massive black hole feedback can heat and/or remove gas from the disk and halo, gas that would otherwise contribute to the formation of the next generation of stars.
8. Thus, an equilibrium state is established as the galaxy goes through a cycle of stellar birth, feedback, gas heating/removal and star formation suppression.

The above processes provide us with a history of galaxy properties. The simulations and models used in TAO are often large, tracking many tens of millions of halos and hence galaxies. It is from the properties contained in such large catalogues that the output of TAO is derived.

3.3. TAO data characteristics

Each simulation and galaxy model will potentially contain a vast array of properties of interest to astronomers. TAO groups its data for each halo–galaxy pair into the following categories:

- Baryonic masses, such as stellar mass, cold gas mass, and hot halo gas. Metals for each baryonic component are included in this category.
- Other galaxy properties, such as the star formation rate, disk scale radius, and cooling and AGN heating rates.
- Halo properties, such as virial mass, radius and velocity, the halo spin vector, and velocity dispersion.

⁴ <https://wiki.asvo.org.au/display/TAOC/Available+Data+Sets>

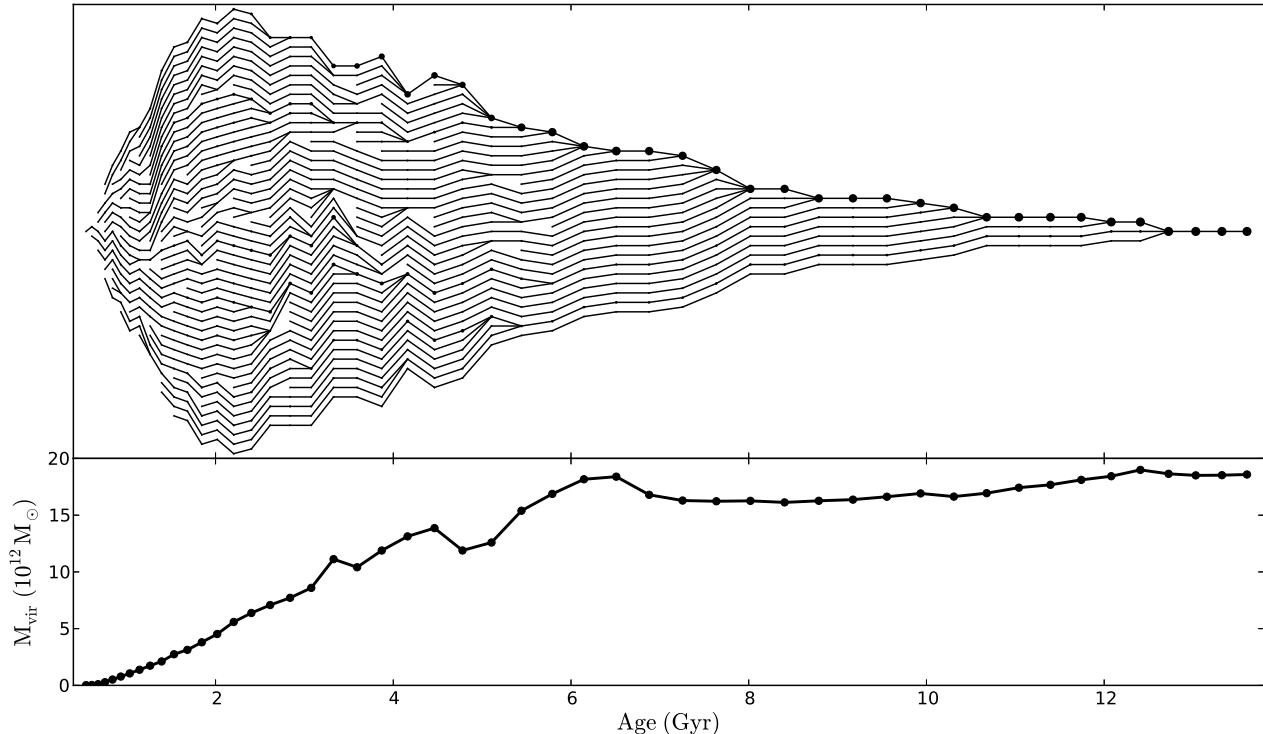


FIG. 3.— A dark matter halo merger tree drawn from the Millennium Simulation (top) and its mass evolution (bottom) with time. This halo has a final mass of $1.9 \times 10^{13} M_{\odot}$ (assuming $h = 0.73$) and would be typical of a group sized system in the real Universe.

- Co-moving positions and physical (peculiar) velocities common to both halos and galaxies. These are always given in the Cartesian coordinate system of the simulation box.
- Additional simulation properties, including the temporal snapshot number and any galaxy and halo IDs.

For those considering importing their data into TAO, in Table 1 we provide a summary of the minimum property requirements that TAO needs to operate, broken down by science module.

Light-Cone Requirements: To build a mock light-cone the data must contain Cartesian coordinates for each halo–galaxy pair from the original simulation box; these are then converted to angular coordinates and redshifts using methods described in Section 4. Furthermore, conversion to redshift space requires Cartesian velocities (i.e. proper motion of the galaxies).

SED Requirements: TAO must be able to walk each halo merger tree from any point in its history. Hence, for each object we require pointers that identify both the previous time-step progenitor and that link the sequence of subhalos in a FoF halo at a given time-step in order of decreasing mass. We adopt the SUBFIND system of pointers, assuming they are stored in depth-first order for each merger tree, as illustrated by Figure 11 of the Supplemental Material in Springel et al. (2005). Furthermore, to calculate magnitudes the SED module must be able to extract star formation and metallicity histories for each galaxy. Also, the initial

mass function (IMF) assumed when calibrating the model is required (e.g., this typically constrains the recycling fraction of mass returned to the interstellar medium from stellar winds).

Mock Image Requirements: The image module requires some measure of morphology to correctly construct the right shape for each galaxy before rendering. This may take the form of separate disk and bulge stellar masses, for example.

3.3.1. Units

We conclude this section by defining the unit and Hubble constant conventions assumed in TAO. The use of little h in particular can differ significantly between the theory and observational communities (and even within a community) and care must always be taken (Croton 2013). Unless otherwise stated:

- Masses adopt $h^{-1}M_{\odot}$.
- Positions adopt $h^{-1}\text{Mpc}$ and are in co-moving coordinates.
- Sizes adopt $h^{-1}\text{Mpc}$ and are in physical coordinates.
- Velocities adopt km s^{-1} and are in physical coordinates.
- Star formation rates adopt $M_{\odot} \text{ yr}^{-1}$.
- Heating and cooling rates are in units of $\log_{10} \text{ erg s}^{-1}$.

| Module | Minimum information required |
|------------------------------------|---|
| Simulation & Model (§3) | <ul style="list-style-type: none"> • A list of the simulation snapshot time-steps. The box size, particle mass resolution and assumed cosmological parameters. |
| Light-Cone (§4) | <ul style="list-style-type: none"> • Co-moving coordinates (x, y, z) and physical (peculiar) velocities (v_x, v_y, v_z) for each halo/galaxy at each time-step. • IDs that associate subhalos/satellites with their parent central halo/galaxy. |
| SED (§5) | <ul style="list-style-type: none"> • Indices connecting the history of each halo/galaxy across time through the galaxy merger tree (see Section 3.3). • Galaxy star formation rate and metallicity at each time-step. • The initial mass function assumed by the galaxy model. |
| Mock Images (§6) | <ul style="list-style-type: none"> • A measure of galaxy morphology, such as independent galaxy disk and bulge stellar masses. • The output from the light-cone and the SED modules. |

TABLE 1
DATA REQUIREMENTS FOR THE TAO MODULES.

- Photometric magnitudes are calculated assuming the h value of the dark matter simulation used to produce the mock catalogue.

4. THE LIGHT-CONE MODULE

N-body simulations of the type discussed in the previous section typically adopt a periodic three-dimensional box geometry. This is in contrast to the geometry observed with a telescope, where galaxies are seen strung out along the observer’s light-cone. Converting between a box and a light-cone for the purpose of building a mock catalogue is a mechanical yet non-trivial task (Blaizot et al. 2005; Kitzbichler & White 2007; Carlson & White 2010). In TAO, this is taken care of by the light-cone module.

The module can work in two modes. The first is to produce light-cones from entirely unique structure, meaning any galaxy can be selected for the cone from any point in its history at most once. This mode is similar to the method described by Carlson & White (2010). In our work we concentrate on automated light-cone construction using an analytic solution for the inclination angle calculations.

The second mode is for larger light-cones. It is used when it is not possible to fill the light-cone volume without repetitions of the structure. This mode is similar to that described in Blaizot et al. (2005). Our algorithm, however, additionally involves random mirroring of the simulation box along the principal axis, increasing the number of pseudo unique volumes by a factor of three. Also, to make the randomised structure even more unique a translation is performed, random shifting along the principal axis. We describe both of these enhancements below.

To explain cone construction, we start with some basic

concepts and build up to the more sophisticated method used by TAO.

4.1. Basic light-cone construction

To build a basic light-cone we place an observer at one of the corners of the simulation box and have them “look out” at the model galaxy distribution. We do this by remapping the Cartesian coordinates of each galaxy into their angular positions in right ascension (RA), declination (Dec) and radial distance (d). This operation defines the basic cone geometry in real-space.

$$\begin{cases} d = \sqrt{x^2 + y^2 + z^2} \\ \text{RA} = \arctan\left(\frac{y}{x}\right) \\ \text{Dec} = \arcsin\left(\frac{z}{d}\right) \end{cases} \quad (1)$$

Here x , y , and z are the co-moving coordinates along the principal axes of the simulation box.

For TAO to provide a redshift for each galaxy on the cone it is necessary to invert the radial distance, d , using the distance–redshift relation for the given simulation cosmology (Hogg 1999). This is defined by

$$d = d_H \int_0^z \frac{dz'}{E(z')}, \quad (2)$$

where $d_H = c/H_0$ is the Hubble distance, c is the speed of light, H_0 the Hubble constant, z is now redshift, and the expansion factor $E(z)$ is defined as

$$E(z) \equiv \sqrt{\Omega_M(1+z)^3 + \Omega_k(1+z)^2 + \Omega_\Lambda}. \quad (3)$$

Ω_M , Ω_k , and Ω_Λ are the matter density, curvature, and cosmological constants, respectively. To obtain the real-space (i.e. cosmological) redshift z , TAO simply inverts Equation 2.

However TAO also has the capacity to generate cones in redshift-space, meaning with line-of-sight peculiar velocities factored into the radial distance. To determine the redshift-space (i.e. observed) redshift for each galaxy, z_{obs} , we solve

$$(1 + z_{\text{obs}}) = (1 + z)(1 + z_{\text{pec}}), \quad (4)$$

where z is the real-space redshift from above, and $z_{\text{pec}} = v_{\text{pec}}/c$ is the redshift distortion due to the objects peculiar velocity v_{pec} , given by

$$v_{\text{pec}} = \left(\frac{x}{d}v_x + \frac{y}{d}v_y + \frac{z}{d}v_z \right). \quad (5)$$

Here v_x , v_y , and v_z are the physical coordinates of the velocity for the galaxy in km/s. As such, each TAO galaxy returns a cosmological redshift (real-space, from Equation 2) and an observed redshift (redshift-space, from Equation 4), based on its position and dynamics in the cone.

4.2. Expanding the cone beyond the box

A problem with the above cone construction becomes apparent when building cones that are deeper in radial extent than the box from which the cone is cut. However, there are a number of ways to deal with this. All of them rely on the fact that most modern simulations are run assuming periodic boundary conditions, meaning that each side of the box connects seamlessly with

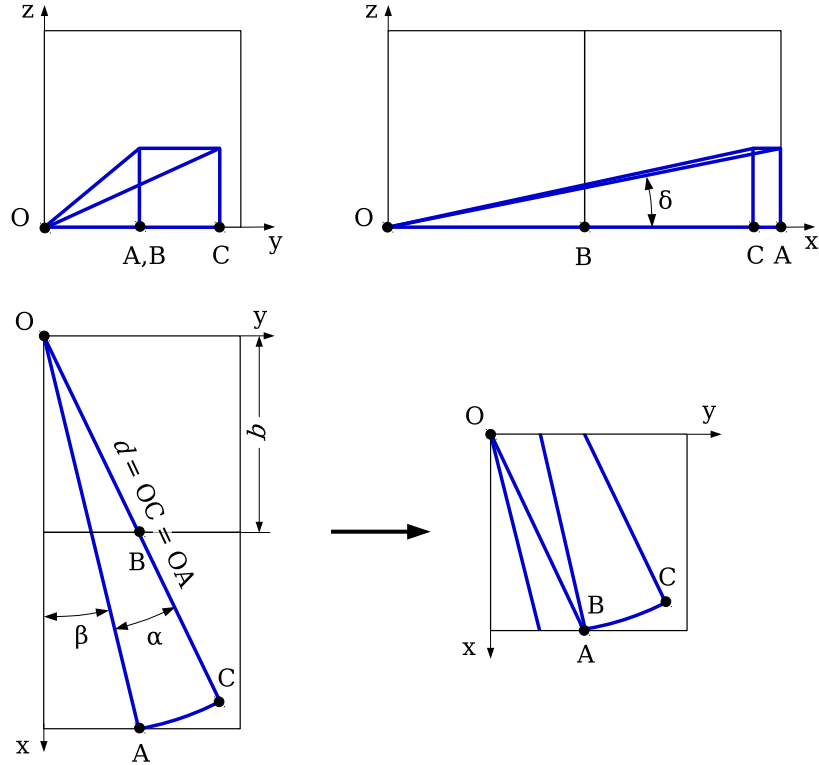


FIG. 4.— The geometry related to finding a unique light-cone path through a replicated simulation cube with side-length b , projected in each Cartesian plane (upper two and lower-left panels). The user-selected cone opening angles are marked by α for RA and δ for Dec. β is the RA translation TAO must find to ensure the cone volume never overlaps as it extends a distance d through the boxes. A, B and C mark points in the last replicated simulation box used in Equation 7. Once a non-overlapping (i.e. unique) path is found, the boxes are collapsed back to a single box (lower-right panel) and the entire simulation is rotated so-as to point the cone at the requested area of the sky. See Section 4 for a full description.

its opposite side. Periodic boundary conditions are a requirement for all simulation data in TAO. There are now two cases to consider.

4.2.1. Unique cones

To construct a unique extended cone we replicate the box in the desired direction and continue the cone construction into this ‘new’ box. To ensure the cone is unique – i.e. any given galaxy in the box along any point in its history is only featured in the cone at most once – we carefully select the angle the cone initially cuts through the box so that it never overlaps with itself as it extends. A similar method is used in Carlson & White (2010). Here we present an analytical method to find the optimal (or at least sufficient) unique path.

In Figure 4 we present three projections of an extended box and the desired unique volume through it. Note that initially we ignore the absolute direction in RA and Dec the user has chosen for their unique cone; later we will rotate the entire simulation appropriately so that the found unique volume points at the requested patch of sky, correctly accounting for declination effects.

The angles α and δ in Figure 4 represent the cone opening angles in the RA and Dec planes respectively, taken from the minimum and maximum angles requested by the user. To find the unique volume we need to determine the angle β (confined to the RA plane), which is the required cone offset such that, as the cone extends back through the replicated boxes, there are no intersections

with any previous volume, as illustrated.

First, the following two minimal conditions must be met:

$$\begin{aligned} d \sin(\alpha + \beta) &\leq b, \\ d \sin(\delta) &\leq b. \end{aligned} \quad (6)$$

In other words, at its furthest end, d (from Equation 1), the opening width of the cone in both directions cannot be larger than the width of the simulation box, b . Otherwise we may be extending into volume that the method cannot guarantee is unique.

Second, considering the lower-left panel in Figure 4 which looks down onto the RA plane, the length along the y-axis from 0 to B must be shorter than or equal to the length along the y-axis from 0 to A, as marked. This requirement ensures that, when the cone path through the replicated boxes is collapsed back to a single box, as shown in the lower-right panel, that point A does not lie inside the earlier part of the cone marked by point B. This only needs to be true for the *last replicated box* where the arclengths are the widest. This requirement can be written

$$d \sin(\beta) \geq OB \sin(\alpha + \beta), \quad (7)$$

where $OB = d - BC$, and BC can be found using the law of sines: $BC = b \sin(90 - \alpha/2 - \beta)/\sin(90 - \alpha/2)$. If a β value satisfying these conditions can be found the cone is unique. Otherwise, the user is asked to either

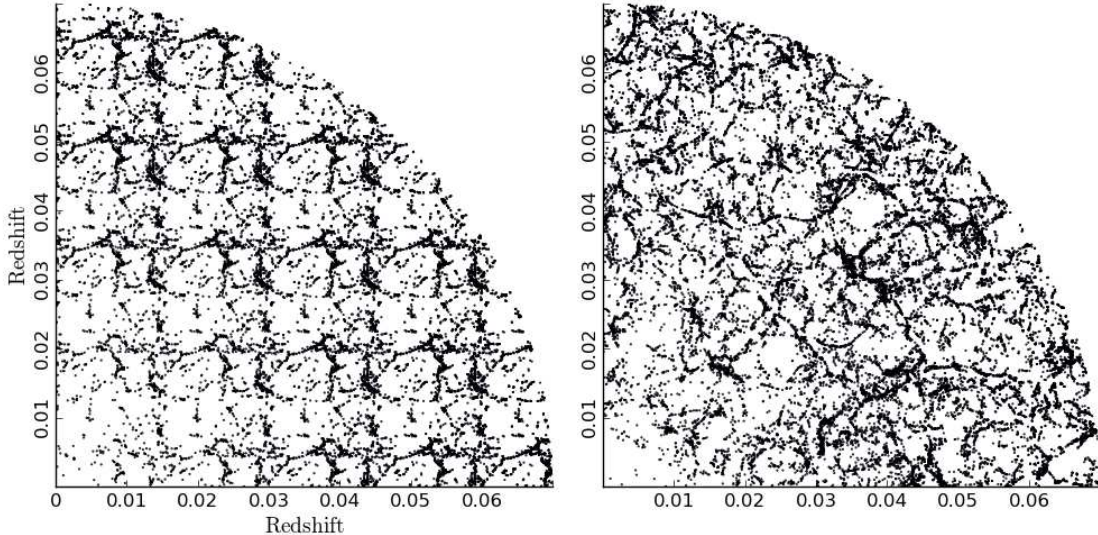


FIG. 5.— Two volume limited light-cones built from a simulation with a box side-length of $62.5 h^{-1}$ Mpc. The left cone shows the result of standard box replication, while the right cone includes the random rotation, shifting and mirroring techniques employed by TAO to minimise any periodicity, as discussed in Section 4.2.2.

modify their cone parameters or consider a ‘random’ cone (described below).

Finally, to complete the cone we apply an equatorial coordinate system to the unique volume, orientated such that the cone points in the direction on the sky specified by the minimum and maximum RA and Dec requested by the user. Galaxies within the requested range and depth are then drawn from the volume and added to the unique cone.

We note that with TAO one can build a unique *full-sky* catalogue by constructing 4 unique light-cones with opening angles 90×90 degrees² and with a depth of up to half of the side length of the simulation box. These 4 cones can then be combined by the user in post-processing, placing the observer at the origin to provide an all-sky view of the theoretical ‘sky’.

4.2.2. Random cones

More typically, however, the volume of the desired cone is larger than the volume of the simulation cube. In this case one can build a random cone. Although such cones result in the replication of structure, any periodicity can be mitigated somewhat by using randomisation techniques (e.g. Blaizot et al. 2005) which produce a more realistic light-cone with pseudo-unique structure (i.e. repeated but non-periodic).

To remove the appearance of periodically repeating structures three randomisation transformations are applied within the TAO light-cone module: random rotation, mirroring, and translation of each repeated simulation cube.

Rotation: The rotation matrix of the principal axis x , y and z is given by

$$\begin{bmatrix} x' \\ y' \\ z' \end{bmatrix} = \begin{bmatrix} \hat{\mathbf{u}}_x & \hat{\mathbf{v}}_x & \hat{\mathbf{w}}_x \\ \hat{\mathbf{u}}_y & \hat{\mathbf{v}}_y & \hat{\mathbf{w}}_y \\ \hat{\mathbf{u}}_z & \hat{\mathbf{v}}_z & \hat{\mathbf{w}}_z \end{bmatrix} \begin{bmatrix} x \\ y \\ z \end{bmatrix} \quad (8)$$

$$\begin{cases} \hat{\mathbf{u}}_x = \cos \theta \cos \psi \\ \hat{\mathbf{u}}_y = \cos \theta \sin \psi \\ \hat{\mathbf{u}}_z = -\sin \theta \end{cases} \quad (9)$$

$$\begin{cases} \hat{\mathbf{v}}_x = -\cos \phi \sin \psi + \sin \phi \sin \theta \cos \psi \\ \hat{\mathbf{v}}_y = \cos \phi \cos \psi + \sin \phi \sin \theta \sin \psi \\ \hat{\mathbf{v}}_z = \sin \phi \cos \theta \end{cases} \quad (10)$$

$$\begin{cases} \hat{\mathbf{w}}_x = \sin \phi \sin \psi + \cos \phi \sin \theta \cos \psi \\ \hat{\mathbf{w}}_y = -\sin \phi \cos \psi + \cos \phi \sin \theta \sin \psi \\ \hat{\mathbf{w}}_z = \cos \phi \cos \theta \end{cases} \quad (11)$$

where ϕ , ψ and θ are Euler angles. For the sake of performance TAO randomly takes values of 0, 90, 180 or 270 degrees.

Mirroring: Mirroring of the simulation volume can be simply achieved by changing an axis direction. It should be noted that inversion of all of the principal axis in combination with rotation may result in the original positions in the simulation cube, so these combinations are excluded from the randomisation routine.

Translation: To translate the cube we cut the simulation box at a random position along one axis and move the sliced volume before this position to the end of the simulation box along of the same axis. This operation doesn’t affect continuous structure in the box because of the periodic boundary condition in the original simulation.

To illustrate the effects of replication and randomisation we construct two mock light-cones built with TAO using the milli-Millennium Simulation (Springel et al. 2005) having box side-length $62.5 h^{-1}$ Mpc. This is

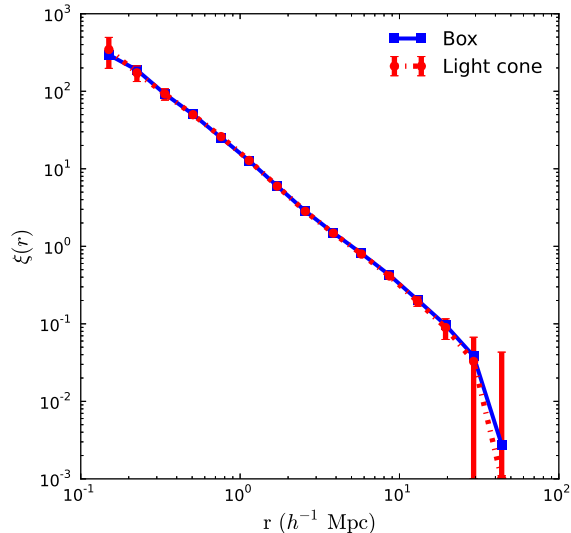


FIG. 6.— The galaxy 2-point correlation function measured in the original Bolshoi simulation box (blue solid line), and from 20 randomised mock light-cones constructed using the box and the procedures described in Section 4 (red dashed line). Error bars represent the 3σ scatter amongst the 20 cones, and highlight the level of consistency between the box and cone results.

shown in Figure 5. The first assumes straight replication of the simulation box (left panel), while the second applies the above random rotations, shifting and mirroring (right panel).

The differences between the left and right panels of Figure 5 are striking. At a bare minimum, given the visual nature of astronomical research clearly non-periodic mock catalogues are desirable. But more importantly, randomisation removes the possibility of unintended replicated features creeping into statistical applications of the mock. We emphasise however that spatially-dependent results should never be drawn from mocks on scale-lengths larger than the simulation box itself.

To quantify the effect of such operations on the spatial distribution of galaxies along the cone, in Figure 6 we plot the real-space 2-point correlation function for galaxies drawn from TAO that are more massive than $10^{10} h^{-1} M_{\odot}$. We first do this for original galaxy positions in the the Bolshoi simulation box (Klypin, Trujillo-Gomez & Primack 2011), which has a side-length of $250 h^{-1} \text{Mpc}$ (solid blue line). We then compute the clustering in 20 cones cut from the same (full) simulation box, each with an area of 30×30 degrees on the sky covering redshift $0 < z < 0.2$ (up to $576 h^{-1} \text{Mpc}$ depth along the line-of-sight, dashed red line). This selection ensures that volumes are similar for both cones and the box. Each of the cones span six replicated boxes and therefore include all three random transformations described above. The 3σ scatter in the clustering results are used as a measure of the clustering uncertainty in the generated cones sample, shown by the error bars. Figure 6 shows consistent behaviour between the original galaxy distribution and randomised cones across the range of scales plotted.

4.3. Time evolution along the cone

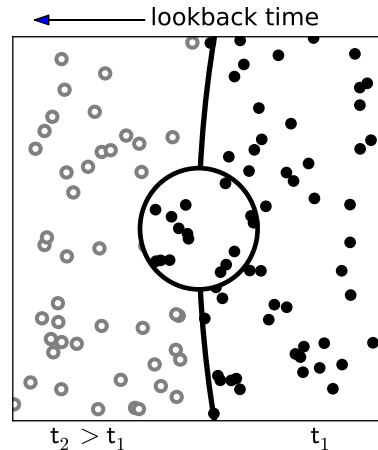


FIG. 7.— Subhalos from the same parent dark matter halo on a border between two redshift zones are kept together. The open dots show the galaxy positions from the previous time-step in the simulation, whereas the solid circles show galaxies from the next time-step. The large circle in the middle defines the region occupied by one particular dark matter halo, which we preserve from splitting when applying time evolution across the cone galaxies.

As we progressively move back through the light-cone away from the point of observation we see galaxies from earlier and earlier epochs, due to the time required for the light from each galaxy to cover the distance. Therefore, to construct an accurate cone we need to not only worry about the spatial distribution of the galaxies in it, but their evolution as well. Remembering that a galaxy’s radial distance can be directly mapped to a cosmic time, we place each galaxy in the cone as it appeared in the simulation at the age of the Universe corresponding to the distance between the galaxy and the observer.

By doing this we also reduce the consequences of structure replication during the cone construction processes. Not only will repeated large-scale structures be seen from different orientations due to the randomisation algorithm described above, but they are likely to be earlier (or later) versions of their duplicates, perhaps appearing differently depending on the growth history of each halo–galaxy system.

There is an additional complication here that is quite subtle yet important, as illustrated in Figure 7. A key part of the light-cone production is to make sure satellite galaxies are always connected to their parent dark matter halo. It often happens that a dark matter halo has its position in the cone very close to the border between different simulation time-steps. If so, satellite galaxies in that halo may inadvertently be split in time across the boundary, and then also be displaced by the randomisation part of the algorithm. In order to provide structural consistency, when building the light-cone, similar to Carlson & White (2010), we group galaxies (centrals and satellites) by their parent halo association as given in the TAO database. Based on the position of the halo centre we then insert these as a unit into the cone, even if the unit spatially crosses the time boundary at any point. This ensures that entire galaxy–halo structures at the same time-step are selected for the cone.

A more advanced technique for interpolating the positions of satellite galaxies is discussed in Merson et al. (2013). However, given the discrete nature of simulation

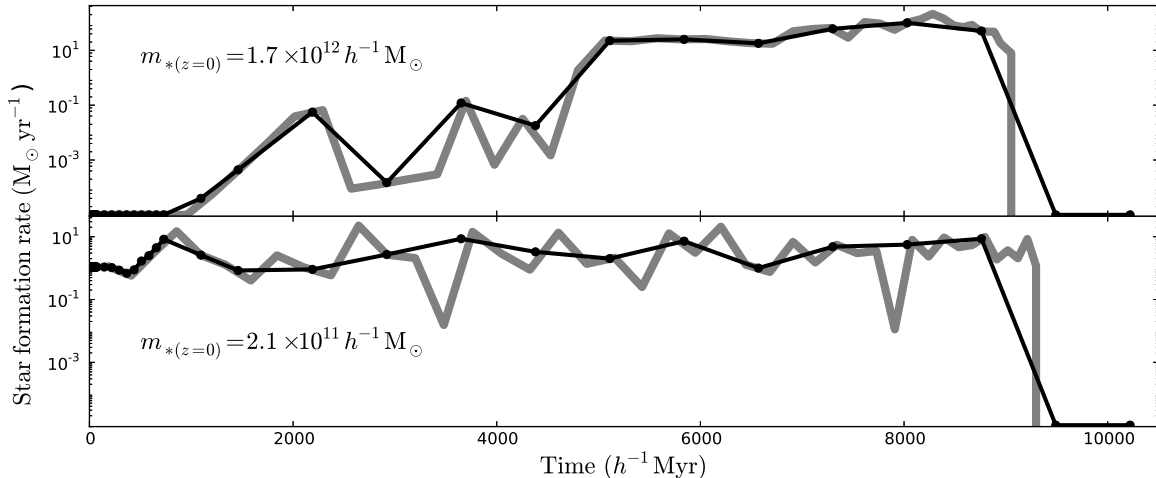


FIG. 8.— Star formation histories of two galaxies in the TAO database: a large elliptical galaxy (top) and a large Milky Way-type spiral galaxy (bottom). For each, the grey thick line shows the original star formation history from the semi-analytic model on the time grid of the dark matter simulation, whereas the thin black line with points indicates the interpolated star formation history on the grid required by the SED module in TAO.

snapshots we have to accept that all galaxy properties, including positions, will reflect only one point in time and are locked to the time-steps of the simulation. A more direct way to reduce the effect of discreteness is to run simulations with higher time resolution, although this will inevitably result in an increased data size that will require more powerful computers with larger storage capacities.

5. THE SPECTRAL ENERGY DISTRIBUTION MODULE

The next crucial step to building mock galaxies is to model their stellar emission, which further enables the translation of theoretical quantities into mock observables. The light emitted by a galaxy is the direct outcome of the formation and evolution of stars, which is regulated by all the physical mechanisms involved in galaxy formation.

From a practical point-of-view, modelling galaxy emission can be separated from the rest of the galaxy formation model. In TAO, this is performed as a post-processing step in the spectral energy distribution module and applied to the TAO galaxy data. This post-processing link uses the prediction for the star formation rate and metallicity of each galaxy at each time step to synthesise galaxy spectral energy distributions at the required time in the galaxy history.

Keeping all records of all star formation episodes for every galaxy can increase the simulation output size significantly. However, thanks to the relational design of the TAO database we can efficiently trace each galaxy history among its progenitors using a system of FOF indexes, described above and in Springel et al. (2005).

Some existing publicly available models offer galaxy luminosities calculated at each simulation time step as the model is run, which are then interpolated according to the final position in the light-cone (Blaisot et al. 2005). Others offer a more sophisticated interpolation with k-correction included (Merson et al. 2013). TAO, in contrast, calculates a more accurate galaxy luminosity directly from spectra constructed ‘on-the-fly’ in post-

processing, using each star formation history starting from the actual galaxy position in the light-cone. This approach also has the advantage of allowing different stellar population synthesis models to be tested with existing galaxy data long after the model was originally run.

5.1. Stellar population synthesis models

Galaxy light is the superposition of the emission of all the stars in the galaxy. A galaxy is composed of a series of single stellar populations (SSPs), i.e. ensembles of stars formed in single episodes with the same age and metallicity. The SSPs that compose a galaxy either originate in the galaxy itself through star formation, or are accreted from satellite galaxies. The emission of every SSP has to be modelled and added to the total galaxy light. Obviously, as the stars in the galaxy age their emission changes with time, and the model needs to take this time-dependance into account.

The tools used to accomplish this are stellar population synthesis (SPS) models, which are libraries of spectra of single stellar populations built on a grid of ages and metallicities, assuming a particular initial mass function (IMF) (e.g. Bruzual & Charlot 2003; Maraston 2005; Conroy, Gunn & White 2009). In order to model the galaxy emission as a function of time, at every time-step in the galaxy model we keep track of all the single stellar populations in the galaxy, then assign them the corresponding emission based on their age and metallicity. We then sum over all populations to obtain the total galaxy light, i.e. its spectral energy distribution (SED). At this stage the complicating contribution of dust extinction and emission must also be included (see Section 5.4).

Semi-analytic models are now taking advantage of such methods to generate galaxy light (Hatton et al. 2003; Tonini et al. 2009, 2010; Henriques et al. 2011; Merson et al. 2013), which add a level of sophistication and flexibility. The use of spectra, as opposed to magnitude tables (De Lucia, Kauffmann & White 2004; Croton et al. 2006; Baugh 2006; Bower et al. 2006) brings a number of advantages: 1) an increased preci-

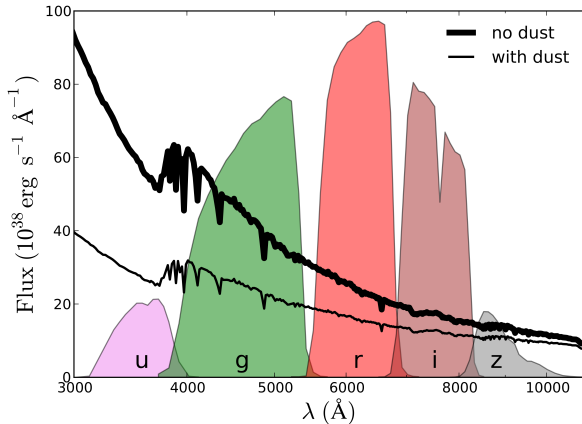


FIG. 9.— Synthetic spectra of a galaxy from TAO at $z = 0$ that has a star formation rate of $15M_{\odot} \text{ yr}^{-1}$ and stellar mass $2.1 \times 10^{10} h^{-1} M_{\odot}$. Here the Maraston (2005) SSP model has been assumed. The thick line shows the spectra without dust extinction, while the thin line is the same but with the dust model from Tonini et al. (2012) applied. Over-plotted are the SDSS u , g , r , i , z transmission functions using an arbitrary y-axis scale.

sion due to the linear additive nature of luminosity *vs* the logarithmic behaviour of magnitudes; 2) an increased accuracy for the determination of observed magnitudes, which are obtained by integration on redshifted SEDs rather than through theoretical k -corrections that rely on toy-model spectra; and 3) an enormous flexibility, introduced when SEDs are modelled in post-processing. Producing galaxy spectra allows us to separate the photometric calculations from the semi-analytic model itself, removing the need to re-run the galaxy model every time we want to change the photometry specifications. This can include different initial mass functions (IMF), dust models, filter sets, mock observational errors, and telescope or survey-specific effects.

5.2. Galaxy star formation histories

To calculate a galaxy SED within TAO we require its star formation history, defined as the stellar populations present in the galaxy at the time of observation τ_0 , characterised by stellar mass, age, and metallicity. These populations include stars formed in the galaxy itself and those that have been accreted from satellites along the merger tree⁵.

We build a two-dimensional age and metallicity grid and collapse onto it the stars formed across the entire tree up to the point of observation (i.e. up to the point τ_0 , when we observe the galaxy on the light cone). Here, each bin represents a single stellar population of a given age and metallicity, and from the SPS libraries we select the corresponding spectrum and weight it by the stellar mass formed. Each of these spectra are then added to the total galaxy light to produce the final SED.

The challenge in the production of the star formation history is the grid itself. SPS models are built to follow the vastly different speeds of stellar evolution. For

example, the emission of a young stellar population is dominated by massive stars and changes on time-scales of ~ 1 Myr, while an old stellar population emits steadily on time-scales of ~ 1 Gyr, with emission dominated by less massive main-sequence stars. The star formation history grid needs to provide information on corresponding time-scales in order to produce realistic galaxy SEDs. In particular, the ultra-violet and optical part of the SED is heavily (if not entirely) determined by young stellar populations, an issue that becomes extremely important at high redshifts.

To this end, the star formation histories of every galaxy in the light-cone must be written by TAO onto a time-varying grid, anchored at the time of observation τ_0 , being finely spaced (steps of 1 Myr) for young ages near τ_0 and more sparsely spaced towards older ages. Unfortunately, the intrinsic semi-analytic model time grid (the snapshots on which the model calculates its physics) is not typically spaced like this. For example, the average time step of a model built using the Millennium Simulation is of the order of ~ 300 Myr. Furthermore, refining a galaxy model grid to the level of precision required by SPS models is not usually practical due to the huge amount of data storage that would be required.

To make up for the loss of information on smaller time-scales we spread the time-weighted stellar mass produced in each larger semi-analytic model output step onto the fine SPS time grid close to τ_0 . Note that this is equivalent to assuming that in each simulation time bin we have a constant star formation rate. At the other end of the SPS time grid the opposite is done, where the mass produced across multiple model time-steps are collected and re-binned to fill the coarser SPS grid, accounting for the slow evolution of the old stellar populations.

In Figure 8 we plot two example star formation histories from a semi-analytic model in TAO, one for a spiral galaxy and one for an elliptical. In both panels, the *grey line* represents the galaxy star formation rate binned using the original simulation time grid, summed over all the branches in the merger tree, while the *black line* represents the star formation history interpolated over the SPS time grid used in TAO. Notice how, for recent times (i.e. close to τ_0), the spacing of the SPS grid is very fine, and the interpolation recovers the SAM star formation history exactly, while for older ages the spacing becomes sparser, providing an approximated reconstruction.

5.3. Galaxy spectro-photometric properties

TAO produces galaxy photometry after determining the SEDs. Magnitudes are calculated by convolving each galaxy spectrum with a set of filter transmission functions, which include filters from many of the most commonly used instruments and surveys. TAO interpolates filters and spectra on a variable wavelength grid so that the resolution of the integration is constant no matter the wavelength extension of the filter function.

The user is given the choice of both absolute and apparent magnitudes for each filter. In the case of absolute magnitudes, fluxes are calculated from the total luminosity on a sphere of radius $R = 10\text{pc}$. For apparent magnitudes, the flux is calculated on a sphere of radius equal to the luminosity distance corresponding to the redshift of the galaxy. The spectrum is dimmed and stretched in wavelength according to the redshift, and then con-

⁵ As an aside, the capacity to record the star formation history of a galaxy in its actual merger tree is an undeniable advantage of semi-analytic models over many other models techniques: without the merger tree information toy-models of galaxy evolution can not account for the complexity of the hierarchical nature of the galaxy assembly, potentially introducing significant biases (Tonini et al. 2012).

volved with each selected filter function. Notice that this operation is exact, as opposed to the approximation of using a k-correction, as both the rest-frame and observed (stretched) spectra are known.

In Figure 9 we show an example SED from a $z = 0$ star forming galaxy in TAO (thin line), where the Maraston (2005) SPS was chosen. It is evident that recent and more intense star formation increases the stellar emission in the UV and optical wavelengths, and the young stellar populations dominate the bolometric luminosity. Also shown is the effect of including the contribution of dust extinction (in the UV/optical) and emission (mid-to-far infrared; thin line). The inclusion of dust in the theoretical spectra is available to the user as an option within the TAO SED science module, which we now discuss.

5.4. Dust

Dust emission and extinction plays a fundamental role in shaping the galaxy SEDs, especially in cases of significant star formation, which is particularly relevant at high redshifts. In TAO, we provide dust modelling as a separate step and allow the user to choose whether to apply dust to the galaxy SED or not. Two popular models are available in TAO and are described below.

5.4.1. Slab model

In the slab model, stars and dust are assumed to be homogeneously distributed in an infinite plane-parallel slab with the same vertical scale. The dust-attenuated luminosity at wavelength λ , L_λ^{obs} , is given by

$$L_\lambda^{\text{obs}} = L_\lambda^{\text{intr}} \frac{1 - e^{-\tau_\lambda^{\text{eff}} \sec i}}{\tau_\lambda^{\text{eff}} \sec i}, \quad (12)$$

where L_λ^{intr} is the intrinsic luminosity of the disc and i is its inclination angle. We define the effective dust opacity as $\tau_\lambda^{\text{eff}} = (1 - \omega_\lambda)^{1/2} (1 + z)^{-1/2} \tau_\lambda$, where τ_λ is the face-on dust opacity. Following Devriendt, Guiderdoni & Sadat (1999), τ_λ is expressed as a function of the neutral hydrogen column density of the disc, N_{H} :

$$\tau_\lambda = \left(\frac{A_\lambda}{A_V} \right)_{Z_\odot} \left(\frac{Z}{Z_\odot} \right)^s \left(\frac{N_{\text{H}}}{2.1 \times 10^{21} \text{ atoms cm}^{-2}} \right). \quad (13)$$

Here $(A_\lambda/A_V)_{Z_\odot}$ is the extinction curve for solar metallicity Z_\odot (see Mathis, Mezger & Panagia 1983) and varies with gas metallicity Z and wavelength such that $s = 1.35$ for $\lambda > 2000\text{\AA}$, and $s = 1.6$ for $\lambda < 2000\text{\AA}$ (see Guiderdoni & Rocca-Volmerange 1987 for more details).

The first term of the dust opacity, $(1 - \omega_\lambda)^{1/2}$, accounts for scattering effects, where ω_λ is the albedo. The second term of Eq. 13, often used in semi-analytic models (e.g. Kitzbichler & White 2007, Garel et al. 2012), introduces an additional scaling of the dust-to-gas ratio with redshift which is in broad agreement with observational trends seen in high redshift galaxies, e.g. Reddy et al. (2006).

5.4.2. Calzetti prescription

The dust content of a galaxy can be parameterised with the colour excess $E(B - V)$, which is defined as a normalisation of the spectrum. Physically, dust content

is associated with the presence of Type II supernovae, which are the main contributors to the metals that constitute the dust grains. Such grains are short-lived (with a life-span of the order of $\sim 10 - 100$ Myr), so it is sensible to associate the dust content with the instantaneous star formation rate in the galaxy (see Tonini et al. 2011):

$$E(B - V) = R_{\text{dust}} A \cdot \left(\frac{\dot{m}_*}{\dot{m}_{*,0}} \right)^\gamma + B. \quad (14)$$

Here, $A = (e^3 - e^{-2})^{-1}$, $B = -Ae^{-2}$, $\dot{m}_{*,0} = 1.479 M_\odot \text{y}^{-1}$, and $\gamma = 0.4343$ are values obtained with a calibration of the GOODS sample discussed in Daddi et al. (2007) and the Andromeda galaxy. We use a Calzetti extinction curve, which produces absorption blue-wards of the Johnston K band, and re-emission red-wards (see Calzetti 1997 and Calzetti 2001).

6. THE MOCK IMAGE MODULE

In addition to the spectral energy distribution of individual galaxies or other objects, many astronomical instruments take images of the wider sky in selected parts of the electromagnetic spectrum using broad or narrow filters. Having the ability to model such images with synthetic data provides an important link in understanding how galaxy properties are connected with their observation.

However, fairly comparing images made from different simulations and models can be problematic, and the size of such datasets poses additional challenges for image generation. Consistency when making images is essential to minimise artificial differences due to the underlying simulation data and processing. With this in mind, TAO is able to produce mock telescope images in a consistent, seamless, and user friendly way.

The TAO image generation module uses the SkyMaker software package (see Bertin 2009 for further details). This software takes data produced by the light cone and SED modules and creates realistic telescope images that include many of the usual observational effects, like telescope aperture, optical defects, sky characteristics, and aureole around bright galaxies.

TAO users can request multiple images per submitted job. Each image requires the following parameters:

- the desired bandpass filter out of those chosen in the SED module,
- the observed magnitude limits of galaxies to include,
- the RA and Dec coordinates to centre the image on,
- the opening angles of the image within the light-cone area,
- the redshift range of galaxies to include, and
- the resolution of the final output image file.

To construct an image the module requires information about galaxy positions in the light-cone, galaxy morphology, and total magnitudes in the requested filters. From the bulge and the disk properties SkyMaker renders galaxies, using a de Vaucouleurs profile for the bulge

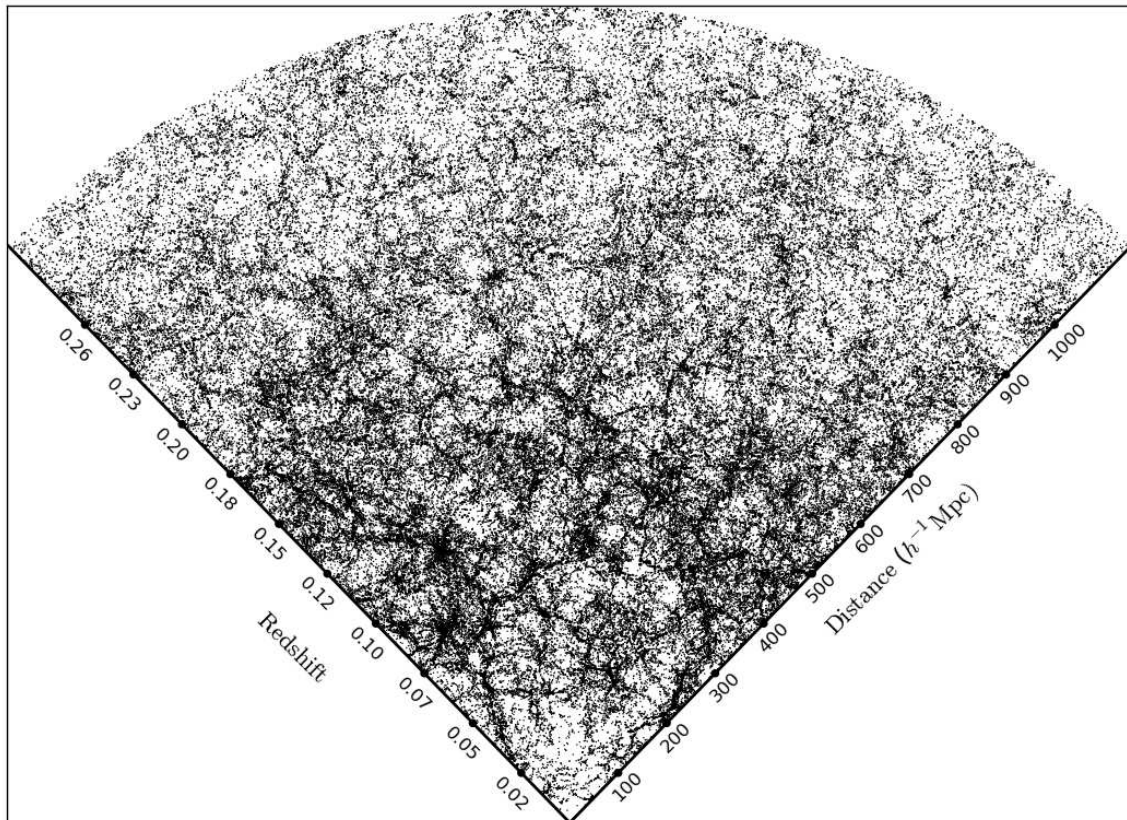


FIG. 10.— A local SDSS-type galaxy mock catalogue with a limiting magnitude of $r < 17.77$, constructed using TAO as described in Section 7.1.

and an exponential profile for the disk. Each galaxy is then placed in the field-of-view to build up the final image.

The point spread function model used in SkyMaker is a convolution of the following components: atmospheric blurring for ground-based instruments⁶, telescope motion blurring, instrument diffraction and aberrations, optical diffusion effects, and intra-pixel response. Sky background, noise, saturation, and quantisation modelling are also added by SkyMaker to reflect the inherent noise and artefacts in charge-coupled devices (CCDs).

Some parameters, like image pixel size and average filter wavelength, are calculated by TAO during job processing. Others are pre-chosen to produce the best image quality; in Table 2 we list these. Any further parameters not listed are kept at their default value, as assumed in the SkyMaker software package (Bertin 2009). As the TAO system develops we will add further customisation options to the user interface for more precise image generation control.

7. EXAMPLES OF MOCK CATALOGUES

There are many ways in which TAO mock catalogues can be built using the tools described so far. One example is the work of Duffy et al. (2012) to make predictions for the Australian Square Kilometre Array Pathfinder (ASKAP) telescope neutral hydrogen surveys of WAL-

⁶ Atmospheric blurring is not currently used in TAO since the default instrument is the Hubble Space Telescope, however ground-based instruments will be added in a subsequent update.

| Parameter | Value |
|----------------------------------|-----------------------------|
| Exposure time | 300 sec |
| Magnitude zero-point | 26 mag |
| Background surface brightness | 50 mag arcsec ⁻² |
| Range covered by aureole | 50 pixels |
| Aureole surface brightness | 16 mag arcsec ⁻² |
| PSF oversampling factor | 7 |
| PSF mask size | 512 pixels |
| Diameter of the primary mirror | 3.5 m |
| Diameter of the secondary mirror | 1 m |

TABLE 2
SKYMAKER DEFAULT SETTINGS IN THE MOCK IMAGE MODULE
INITIAL TAO RELEASE. WITH TIME THESE WILL BE ADDED TO THE
MODULE INTERFACE FOR CONTROL BY THE USER.

LABY and DINGO. TAO comes with an expanding set of popular survey presets, which can be run as-is or used as a template for more specific requirements. To illustrate the utility of TAO, in this section we outline what we expect is a common use case, to build a representation of the local universe as a light-cone and then image a particularly massive cluster of galaxies within its borders.

7.1. SDSS mock catalogue light-cone

One of the largest observational extragalactic databases to date is the Sloan Digital Sky Survey (SDSS) catalogue⁷ (Abazajian et al. 2003; Ahn et al. 2012). The SDSS main catalogue covers approximately

⁷ <http://www.sdss3.org/dr9/scope.php>

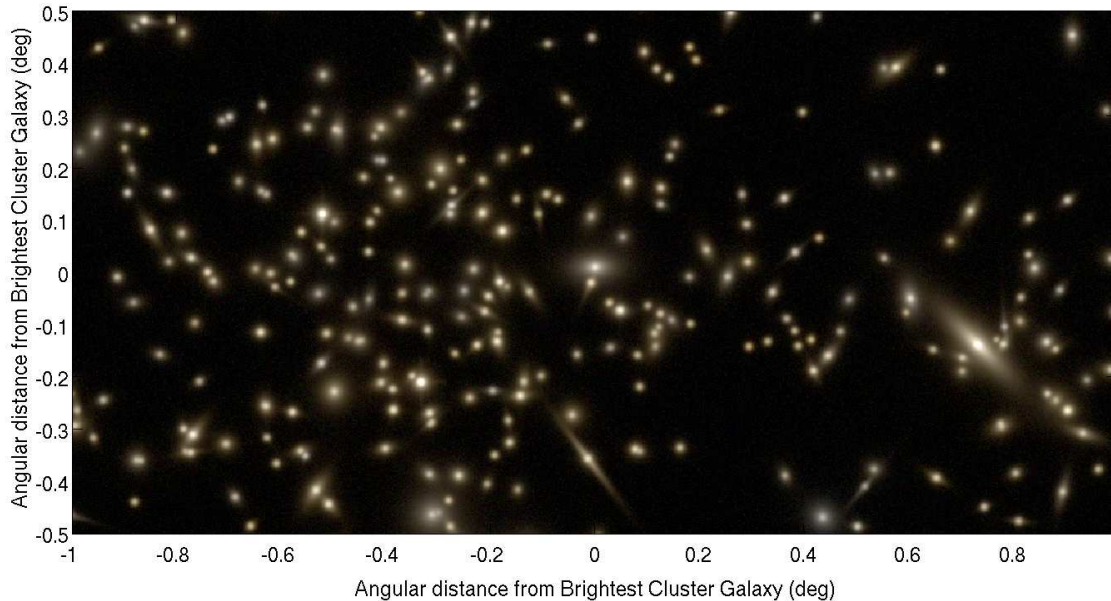


FIG. 11.— An SDSS-*gri* composite image of a $M_{vir} = 5.71 \times 10^{14} h^{-1} M_{\odot}$ galaxy cluster at $z = 0.08$, within a 2×1 degree field-of-view, rendered using the TAO image module as described in Section 7.2. This particular cluster contains 119 galaxies brighter than a limiting galaxy magnitude of $r = 17.6$.

14000 square degrees of the sky across a redshift range $0 < z \lesssim 0.4$. Many thousands of papers have been written using SDSS data, making it the highest impact repository for extragalactic science in the history of astronomy. Hence, the SDSS is a natural place to start if one wants to construct mock analogues of the local universe.

To reconstruct an SDSS volume using TAO we perform the following steps:

- **General Properties:** We select a light cone geometry, then a simulation and galaxy formation model. Here, the Millennium simulation (Springel et al. 2005) and SAGE galaxy model (Croton et al. submitted) are adopted. The RA and Dec opening angles are chosen to be 90 and 60 degrees, respectively, with a redshift range of $0 < z < 0.3$.
- **Spectral Energy Distribution:** For this particular cone we select a BC03 stellar population model assuming a Chabrier initial mass function. All filters marked with ‘SDSS’ are included for output – u , g , r , i , z – both apparent and absolute. We apply the Calzetti dust model described in Tonini et al. (2012).
- **Selection:** Our cone is chosen to be volume limited by including all galaxies with stellar masses greater than $10^8 h^{-1} M_{\odot}$.

After processing, TAO sends an email to the user with a link to the constructed light cone for download. This particular cone contains 3,122,823 galaxies. In Figure 10 we plot these galaxies to illustrate their spatial distribution. The catalogue also contains as many galaxy properties as predicted by the model and requested by the user. Furthermore, the exact same cone can be reconstructed using a different model in the database, or with

a different underlying simulation. This provides the user with an estimate of the theoretical uncertainty between different models and simulations.

7.2. Imaging a local galaxy cluster

We can use the SDSS light-cone constructed above to extend our exploration of the local galaxy volume beyond the spectroscopic. This can be done by employing the TAO image module to predict what an imaging survey might see within the cone.

To this end, from the history page we download the SDSS light-cone data to a local machine and identify the most prominent galaxy cluster within its volume. We define this to be the dark matter halo with the largest galaxy membership (central+satellites) brighter than a limiting magnitude of 17.6 in the r -band (but other selections are of course possible). The winning halo was found at $z = 0.08$, had a virial mass of $5.71 \times 10^{14} h^{-1} M_{\odot}$, and contained 119 galaxies. We note the angular position of the cluster centre and its extent on the sky, both in RA and Dec.

Once identified, the mock image module can be used to build a realistic SDSS-*gri* visualisation to be compared with observations. Within the TAO interface, we revisit the SDSS light-cone data through the history page. From the options presented we choose to image the cone. We then centre our image on the centre of the cluster, select a field-of-view of 2×1 degrees to capture its surrounding environment, and take the full redshift depth of the cone, $0.0 < z < 0.3$, which allows us to model the effect of interlopers. This is done individually for each of the g , r , and i filters to produce three images. We keep most of the SkyMaker imaging options fixed at their default values, with the exception of matching the SDSS exposure time of 53.9 seconds, and choosing not to populate the image with foreground stars.

After processing by TAO we are again notified via

email that our results are ready. The individual g , r and i images are then downloaded and combined to form a single composite image using the ds9 package. This image is shown in Figure 11.

8. SUMMARY

In this paper we have described a new cloud-based virtual laboratory, the Theoretical Astrophysical Observatory (TAO), that enables any astronomer to produce mock galaxy catalogues based on selectable combinations of a dark matter simulation, semi analytic galaxy formation model, and stellar population synthesis model. TAO is built in a modular fashion, starting with the simulation and model database, that flows upward through a series of science modules to connect to the user via a simple web interface.

The key features of TAO are:

- A flexible design with an intuitive web interface that allows public access to many dark matter simulations, galaxy models, and stellar population synthesis models;
- Advanced techniques to create custom mock light-cones of large volumes with realistic structure;
- Galaxy-by-galaxy spectral energy distribution modelling obtained in post-processing, providing accurate galaxy photometry using galaxy star formation and metallicity histories;
- The ability to image light-cone data using the Sky-Maker image processing package, integrated into the TAO workflow.

The flexibility built into TAO make it useful for many applications. Some examples include:

- Making survey predictions and planning observing strategies;
- The comparison of observational data with simulations and models;
- The comparison of different galaxy models run on the *same* dark matter simulation;
- The comparison of a single galaxy model run on *different* dark matter simulations;
- Exploring the effects of different stellar population synthesis models and dust extinction prescriptions on a galaxy's photometric evolution;
- Generating mock images and testing source finding algorithms.

TAO is an open source project and can be freely deployed and further developed by members of the community. The Swinburne TAO portal can also be used by simulators and modellers to make selected data of importance available to the public, which is especially useful when the resources to do this in-house are not available or expensive to implement. Enabling the community with free access to state-of-the-art theoretical data facilitates data reuse and multiplies its value.

ACKNOWLEDGEMENTS

The authors would like to thank Alistair Grant, Jarrod Hurley, Gin Tan, Jennifer Piscionere, and Manodeep Sinha. We also appreciate the time given by the many astronomers who tested TAO during its initial development. Special thanks goes to Andrew Benson for his help importing the Galacticus semi-analytic model into the TAO database. DC acknowledges receipt of a QEII Fellowship by the Australian Research Council (DP1095506). SM, AD and GP are funded from the ARC Laureate Fellowship grant of S. Wytke (FL110100072).

TAO is part of the All-Sky Virtual Observatory and is funded and supported by Astronomy Australia Limited, Swinburne University of Technology, and the Australian Government. The latter is provided through the Commonwealth's Education Investment Fund and National Collaborative Research Infrastructure Strategy, particularly the National eResearch Collaboration Tools and Resources (NeCTAR) project. TAO was constructed as a collaboration between Swinburne University of Technology and Intersect Australia and is hosted on the gSTAR national facility at Swinburne.

The Millennium Simulation was carried out by the Virgo Supercomputing Consortium at the Computing Centre of the Max Planck Society in Garching. It is also publicly available at <http://www.mpa-garching.mpg.de/Millennium/>.

The Bolshoi Simulation was carried out by A. Klypin, J. Primack and S. Gottloeber at the NASA Ames Research Centre. The simulation and data products can additionally be found at <http://astronomy.nmsu.edu/aklypin/Bolshoi/>. The Semi-Analytic Galaxy Evolution (SAGE) model used in this work is a publicly available codebase that runs on the dark matter halo trees of a cosmological N-body simulation. It is available for download at <https://github.com/darrencroton/sage>.

Finally, the authors would like to thank the anonymous referee, whose careful reading of this paper resulted in many valuable improvements.

REFERENCES

- Abazajian K. et al., 2003, AJ, 126, 2081
 Ahn C. P. et al., 2012, ApJS, 203, 21
 Baugh C. M., 2006, Reports on Progress in Physics, 69, 3101
 Behroozi P. S., Wechsler R. H., Wu H.-Y., 2013, ApJ, 762, 109
 Benson A. J., 2012, NA, 17, 175
 Bertin E., 2009, Mem. Soc. Astron. Italiana, 80, 422
 Blaizot J., Guiderdoni B., Devriendt J. E. G., Bouchet F. R., Hatton S. J., Stoehr F., 2004, MNRAS, 352, 571
 Blaizot J., Wadadekar Y., Guiderdoni B., Colombi S. T., Bertin E., Bouchet F. R., Devriendt J. E. G., Hatton S., 2005, MNRAS, 360, 159
 Bower R. G., Benson A. J., Malbon R., Helly J. C., Frenk C. S., Baugh C. M., Cole S., Lacey C. G., 2006, MNRAS, 370, 645
 Bruzual G., Charlot S., 2003, MNRAS, 344, 1000
 Calzetti D., 1997, AJ, 113, 162
 Calzetti D., 2001, PASP, 113, 1449
 Carlson J., White M., 2010, APJS, 190, 311
 Conroy C., Gunn J. E., White M., 2009, ApJ, 699, 486

- Croton D. J., 2013, PASA, 30, 52
Croton D. J. et al., 2006, MNRAS, 365, 11
Daddi E. et al., 2007, ApJ, 670, 156
Davis M., Efstathiou G., Frenk C. S., White S. D. M., 1985, ApJ, 292, 371
De Lucia G., Kauffmann G., White S. D. M., 2004, MNRAS, 349, 1101
Devriendt J. E. G., Guiderdoni B., Sadat R., 1999, A&A, 350, 381
Duffy A. R., Meyer M. J., Staveley-Smith L., Beryk M., Croton D. J., Koribalski B. S., Gerstmann D., Westerlund S., 2012, MNRAS, 426, 3385
Garel T., Blaizot J., Guiderdoni B., Schaerer D., Verhamme A., Hayes M., 2012, MNRAS, 422, 310
Guiderdoni B., Rocca-Volmerange B., 1987, A&A, 186, 1
Hatton S., Devriendt J. E. G., Ninin S., Bouchet F. R., Guiderdoni B., Vibert D., 2003, MNRAS, 343, 75
Henriques B., Maraston C., Monaco P., Fontanot F., Menci N., De Lucia G., Tonini C., 2011, MNRAS, 415, 3571
Hogg D. W., 1999, ArXiv Astrophysics e-prints
Johnston S. et al., 2008, Experimental Astronomy, 22, 151
Keller S. C. et al., 2007, PASA, 24, 1
Kitzbichler M. G., White S. D. M., 2007, MNRAS, 376, 2
Klypin A. A., Trujillo-Gomez S., Primack J., 2011, ApJ, 740, 102
Lemson G., Virgo Consortium t., 2006, ArXiv Astrophysics e-prints
Maraston C., 2005, MNRAS, 362, 799
Mathis J. S., Mezger P. G., Panagia N., 1983, A&A, 128, 212
Merson A. I. et al., 2013, MNRAS, 429, 556
More S., Kravtsov A. V., Dalal N., Gottlöber S., 2011, ApJS, 195, 4
Overzier R., Lemson G., Angulo R. E., Bertin E., Blaizot J., Henriques B. M. B., Marleau G.-D., White S. D. M., 2013, MNRAS, 428, 778
Reddy N. A., Steidel C. C., Fadda D., Yan L., Pettini M., Shapley A. E., Erb D. K., Adelberger K. L., 2006, ApJ, 644, 792
Springel V., 2005, MNRAS, 364, 1105
Springel V. et al., 2005, NAT, 435, 629
Springel V., White S. D. M., Tormen G., Kauffmann G., 2001, MNRAS, 328, 726
Tonini C., Beryk M., Croton D., Maraston C., Thomas D., 2012, ApJ, 759, 43
Tonini C., Maraston C., Devriendt J., Thomas D., Silk J., 2009, MNRAS, 396, L36
Tonini C., Maraston C., Thomas D., Devriendt J., Silk J., 2010, MNRAS, 403, 1749
Tonini C., Maraston C., Ziegler B., Böhm A., Thomas D., Devriendt J., Silk J., 2011, MNRAS, 415, 811
White S. D. M., Frenk C. S., 1991, APJ, 379, 52